Preliminary Assessment of the Soil Foundation Characteristics Utilizing the 2D Resistivity Imaging and Down-Hole Seismic Refraction Techniques: A Case Study in Tenth of Ramadan City, Egypt

Shokry A. Soliman*, Salah Shebl, Ahmed El Khafif, T.F. Shazley, M.H. Farag
Laboratory of geophysics, Egyptian Petroleum Research Institute, Cairo, Egypt

Abstract

Two-dimensional electrical resistivity imaging and seismic refraction, in the form of down-hole survey, were applied to delineate the subsurface section and elastic moduli and identify geotechnical characteristics of subsurface materials in the 10th of Ramadan industrial area, Cairo, Egypt. The results of four 2-D profiles of electrical resistivity, in the form of dipole–dipole and Wenner configurations, revealed that the subsurface section contains two main geo-electrical layers; the first is made of sand, some silt, and gravels, reflecting low resistivity values ranging from 25 to 65.5 ohm m. This layer is overlying a high resistivity layer (65.5 to135 ohm m), corresponding to medium to coarse sand, with gravel and calcareous materials. It is worth noting that that the down-hole technique was used to measure velocities of P and S waves in order to derive the low strain dynamic elastic properties, such as Poisson's ratio, Shear modulus, stress ratio, concentration index, N-value, and the ultimate and allowable bearing capacities of the subsurface soil, down to an approximate depth of 30 m in the borehole at the site. In addition, the Vs30 value was calculated and revealed that the soil is categorized as a NEHRP class (D). Furthermore, the results of geotechnical parameters and elastic moduli were found to be realistic and sensible for the purposes of engineering constructions and imply that the soil in the study area is characterized by fairly to moderately competent quality. A new empirical correlation is proposed between the obtained Vs and resistivity values, where Vs = 1.0302 ρ + 172.74.

Keywords: 2D resistivity imaging, seismic refraction, geotechnical parameters, down-hole, Vs[30]

<div dir="rtl">

التقييم الأولى لخصائص تربة الأساس باستخدام تقنيات المقاومة ثنائية الأبعاد وتقنيات الانكسار الزلزالي دراسةحقلية في مدينة العاشر من رمضان بمصر

شكري سليمان* , صلاح شبل, أحمد الخفيف, طارق شاذلي, محمد فرج

معمل الجيوفيزياء, معهد بحوث البترول المصري, القاهرة, مصر

الخلاصة

تم تطبيق التصوير المقطعي بالمقاومة الكهربائية والانكسار الزلزالي (down-hole) لتحديد الطبقات تحت السطحية ، ومعاملات المرونة وتحديد الخصائص الجيوتقنية للمواد التحت سطحية في المنطقة الصناعية بالعاشر من رمضان. من الضروري إجراء دراسات جيوتقنية قبل أي تصميم هندسي مقترح

</div>

---

*Email: shokry61@yahoo.com

لإنشاء أي مبنى لتجنب انهيار المبنى. لذلك من المهم معرفة الخصائص الجيوتقنية للتربة التي سوف تقام عليها المنطقة الصناعية الجديدة من أجل تنفيذ خطط التنمية لهذه المنطقة. تكشف نتائج أربعة بروفيلات ثنائية الأبعاد للمقاومة الكهربائية في شكل (dipole–dipole and Wenner) أن الطبقات تحت سطحية تحتوي على طبقتين رئيسيتين ؛ الطبقة الأولى تتكون من الرمل وبعض الطمي والحصى والتي تعكس قيم مقاومة منخفضة تتراوح من 25 إلى 65.5 أوم م. تعلو طبقة ذات مقاومة عالية تتراوح من 65.5 إلى 135 أوم م. المطابقة للرمل المتوسط إلى الخشن ، مع الحصى والمواد الجيرية. من الجدير بالذكر ,أنه تم استخدام تقنية (down hole) لقياس سرعات الموجات P)و (S من أجل معرفة خصائص المرونة الديناميكية مثل نسبة بواسون ، ومعامل القص ، ونسبة الإجهاد ، مؤشر التركيز ، قيمة N ، قدرة التحمل النهائية والمسموح بها للتربة الجوفية وصولاً إلى عمق تقريبي يبلغ 30 مترًا في البئر في الموقع. بالإضافة إلى ذلك ، تم حساب قيمة Vs30 وصُنفت التربة على أنها فئة (.D)) علاوة على ذلك ، فإن نتيجة قيم المعاملات الجيوتقنية والمرونة واقعية ومعقولة للإنشاءات الهندسية وتعني أن التربة في منطقة الدراسة تتميز بجودة عالية إلى حد ما. تم اقتراح علاقة جديدة بين قيم سرعة موجات القص والمقاومة الكهربية.

Introduction

A geotechnical study is necessary before any proposed engineering design to construct any building to prevent the building from collapsing. It is important to know the geotechnical properties of the soil on which a new industrial zone, for example, is to be built in order to implement the development plans of this zone. Nowadays, the combination of geoelectrical resistivity and seismic refraction techniques for site investigations is very effective due to their distinct geophysical response with varying resolution. In some geotechnical problems, geophysical studies may be adopted to decide which execution measure should be taken to diminish costs, effort, time, and even the chance of accidents during any constructions.

Several studies used effective geophysical techniques in engineering problems, such as the detection of the ancient foundations, cracks and fractures of building [1, 2], planning on new cities, building new neighborhood, [3-5] and the investigations of shallow subsurface sections, environmental problems and geotechnical parameter [6, 7].

The City of Tenth of Ramadan has been witnessing civil and industrial development represented in constructing new industrial zones, since its establishment in 1977. It is located along the Cairo-Ismailia desert highway about 55 km from Cairo. It lies between latitudes 30°17′ and 30°25′N and longitudes 31°34′ and 31°49′E. The area of study is located within the northeast territory of 10th Ramadan City (Figure 1). The shallow seismic refraction and Dc resistivity were utilized in defining the geotechnical properties of the soil and rocks [8, 9], where shear waves velocity has an intimate relationship with the rigidity or stiffness of the soil or rocks [10], which can be expressed as the elastic shear modulus.

The present study aims to investigate the lateral and vertical variations in the subsurface sections, determine elastic moduli, and identify the geotechnical characteristics of the subsurface soil using integrated 2D electrical resistivity, borehole data, and down-hole (P and S) waves.

Geology of the Study Area

The investigated site and its vicinity are covered by sedimentary rocks (Figure 2) belonging to the Tertiary and Quaternary ages [11]. The subsurface sequences of the uppermost thirty meters of the soil consist of very dense sand, coarse to medium sand, and silty sand (Figure 3), based on the information derived from the two boreholes drilled at the investigated site.
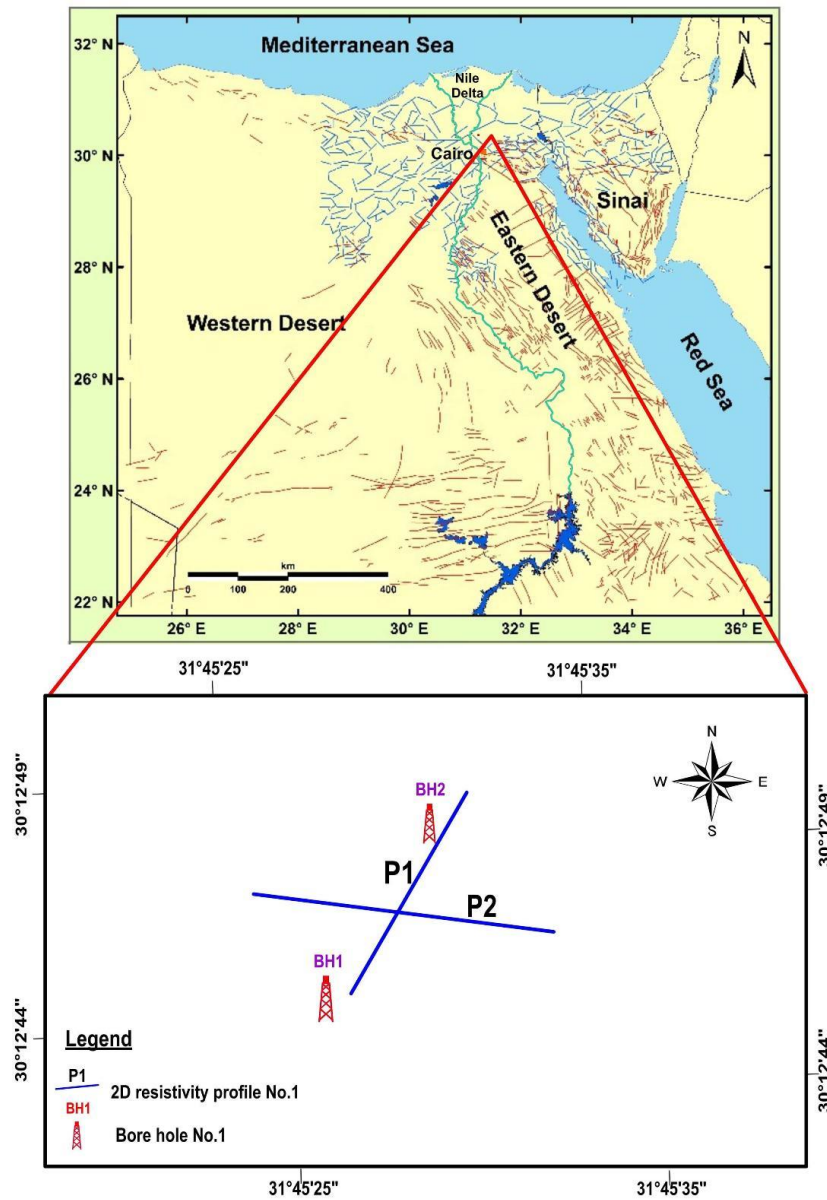
Figure 1- Location map of the study area, electrical resistivity stations, and boreholes sites
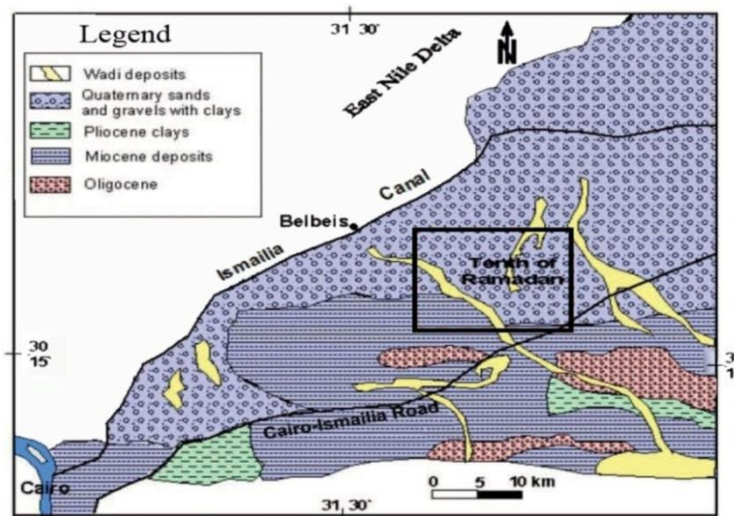

Figure 2- Modified surface geological map of the area and its surroundings [12].
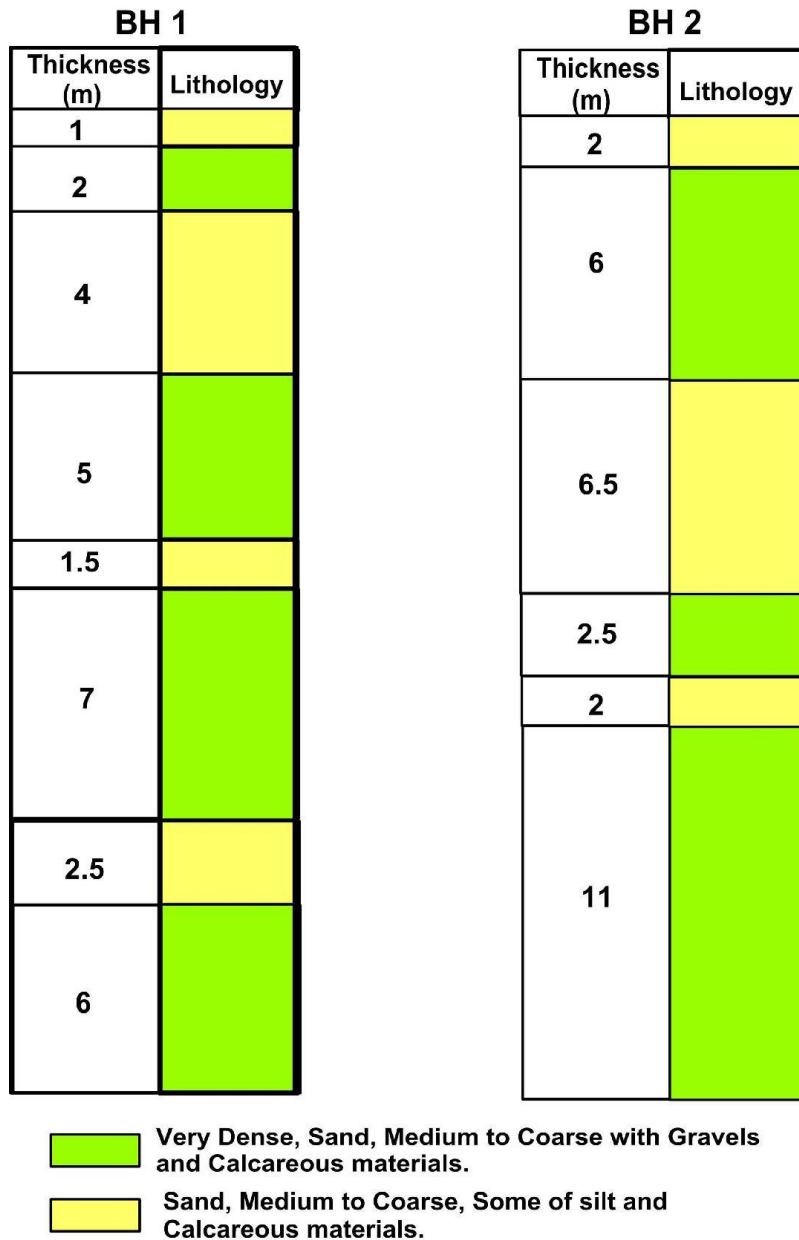
BH 1

Thickness (m)	Lithology
1	
2	
4	
5	
1.5	
7	
2.5	
6	

BH 2

Thickness (m)	Lithology
2	
6	
6.5	
2.5	
2	
11	

Very Dense, Sand, Medium to Coarse with Gravels and Calcareous materials.

Sand, Medium to Coarse, Some of silt and Calcareous materials.

Figure 3- Lithological description of the boreholes BH1 and BH2, [13]

Methodology
2D Resistivity Imaging

The electrical resistivity imaging method was chosen in this study due to its ability to image the subsurface structure and thickness of layers. This technique has wide applications in environmental, engineering, and variable subsurface explorations [14, 15]. Four 2D resistivity profiles were carried out using dipole–dipole and Wenner arrays. The instrument used in the study is SYSCAL-Pro, 48 channels, with an automatic multi-electrode system made by IRIS Instruments, France. The first 2D profile (P1) is located between the two boreholes, while the second profile (P2) is orthogonal on P1 in the study area. Both profiles were measured using dipole–dipole array (Figure 1). In additions, another two profiles of Wenner array were executed at the same locations of dipole–dipole profiles, in order to compare the results of the two techniques. The data were processed and analyzed using RES2DINV program [16], which produces an image of the electrical resistivity distribution in the subsurface based on a regularization algorithm [17].

The inversion routine used by RES2DINV is based on the smoothness constrained least-squares technique [18] which offers three options, providing a very fast quasi Newton method [17]. The program automatically creates a 2D invers model by dividing the subsurface into rectangular blocks and chooses optimum inversion parameters for the data, which include the damping factor, vertical to horizontal flatness filter ratio, convergence limit, and number of iterations. The program calculates the apparent resistivity values of the model blocks using either a finite difference or finite element method and compares these to measured data. The resistivity of the model blocks is adjusted iteratively until the calculated apparent resistivity values of the model agree with the actual field measurements.

Seismic Refraction Tools

Seismic refraction was executed by applying a down-hole technique to measures the compression wave (P) and the shear wave (S) in the borehole using a seismograph model McSEIS-SXW manufactured by OYO Company. During down-hole seismic testing, a seismic source is generated at distance of about 1m from a well. A sledge hammer (10kg) was used to generate both compression (P) and shear (S) waves by striking the loaded plate. Relying on the type of strike plate on the ground surface (vertical or horizontal), the seismic source can generate a signal containing a maximum of energy in the compression wave (P) or the shear wave (S), respectively. Within the borehole, a receiver geophone measured the arrival times by varying its location every 1m until the 30 m depth to determine the P and S wave velocities (Figure 1). The data were recorded and saved as separate files for each shot for both P and S waves corresponding to each depth location.

The down-hole technique is a vital method of the seismic refraction surveys for determining the shear wave velocity and, consequently, estimating the elastic situation (stiffness) of the soil or rock for geotechnical and engineering purposes.

Elastic Moduli and Geotechnical Parameters

The values of P- and S-wave velocities which concluded from the two boreholes measurements were used to evaluate the different elastic moduli, such as density (Eq.1), Poisson's ratio (Eq. 2) [19-21], shear modulus (Eq. 3) [22], Young's modulus (Eq. (4) [23, 24], and bulk modulus (Eq. 5) [25], as listed in (Table 4).

$$\text{Density } (\rho) = \quad \text{o.3Vp.25} \tag{1}$$

$$\text{Poisson's ratio } = \frac{V_P^2 - 2V_s^2}{2(V_P^2 - V_S^2)} \tag{2}$$

$$\text{Shear modulus } (\mu) = \quad \rho VS^2 \tag{3}$$

$$\text{Young's modulus } (E) = 2\mu (1 + \sigma). \tag{4}$$

$$\text{Bulk's modulus } (K = E/3(1 - 2\delta) \tag{5}$$

The Geotechnical Elements

The geotechnical elements, such as the N-value, concentration index, material index, stress ratio, and bearing capacity were evaluated as follows.

N-Value

The N-value is one of the most common geotechnical parameters, known as SPT (Standard Penetration Test). It can be calculated in situ from a well to investigate the status of cohesion-less deposits, where the low competent rocks reveal low N-value and vice versa. The measurements of SPT N values depend on many factors, such as drilling methods, drill rods, borehole properties (e.g. diameter and stabilization, the sampler, blow count rate, hammer configuration, fine content), energy corrections, and test procedure [26,27]. Geophysically, the N-value is determined from the modified equation by [28]

$$Vs = 89.9(N) \ 0.341 \qquad (6)$$

To calculate the N value, this equation can be rewritten as:

$$Log \ N = 2.932log \ VS - 5.7295 \qquad (7)$$

Shear wave data can be converted to SPT N-values, to recognize the type of soil or sediment, and used in calculating bearing capacity. The N-value was originally adopted to investigate the status of cohesionless deposits, but it is widely used in both cohesionless and cohesive deposits for exploration in all types of foundations (Table 1).

Table 1- N-value classes (modified after [29].

Cohesive soil		Cohesionless soil	
N-value	Description	N-value	Description on
<4	Very soft	0–10	Loose
4–6	Soft	11	Medium
7–15	Medium	31–50	Dense
16–25	Stiff	>50	Very dense
>25	Hard		

Table 2- Comparison between SPT N value, shear wave velocity Vs, and Poisson's ratio according to [30-31].

Soil type	SPT N value	S-wavevelocity m/s	Poisson's ratio
Loose granular soil	0–20	130–280	0.2–0.4
Dense granular soil	20–50	200–410	0.3–0.45
Soft clay	0–6	40–90	0.15-0.25
Stiff clay	6–30	65–140	0.2–0.5

Concentration Index

The concentration index is one of the engineering parameters that reveal the degree of the competence of materials used in the foundation and other civil constructions. It depends on two factors; one is the elastic moduli of the substance and the other is depth-pressure distribution [29].

$$C_i = \frac{(3-4\alpha)}{(1-2\alpha)} \qquad (8)$$

Material Index

From the engineering perspective, the material index clarifies the material quality for foundation purposes. This parameter implies the degree of competence based on the elastic moduli. This index depends on several factors, such as matter composition, grade of consolidation, fracturing, jointing, and presence or absence of fluids in pore spaces, which affect the medium of the materials and the wave velocities [29].

$$\xi = (1 - 4\sigma). \qquad (9)$$

Table 3- Soil description according to Poisson's Ratio and Material Index, after [32].

Soil description	Incompetent to slightly competent	Fairly to Moderately competent	Competent Material	Very high Competent
Poisson's Ratio	0.41-0.49	0.35-0.27	0.25-0.16	0.12- 0.03
Material Index	(-0.5)-(-1)	-0.5-0.0	0.0-0.5	>0.5

Bearing Capacity

In geotechnical engineering, the bearing capacity is a gauge for structural stability of the soil. The failure criterion for any foundation soil is known by the ultimate bearing capacity and it is considered an important factor in soil mechanics [23].

Allowable bearing capacity (Qa)

It is defined as the maximum load to be considered to avoid shear failure. It can be reduced from the ultimate bearing capacity value by the value of safety factor (F), according to [33].

$$Qa \qquad \frac{1}{4} \qquad Qult = F \qquad (10)$$

where Qa is the allowable bearing capacity and Fs is the factor of safety (F), which equals three for cohesive soils. This equation can be rewritten in terms of shear velocity in the case of cohesive soils, as follows:

$$\text{Log} \quad Qa \quad = \quad 2.932 \quad \log \quad Vs \quad – \quad 4.729 \qquad (11)$$

For cohesionless soil,

$$LogQa \quad = \quad 2.932 \quad \log \quad Vs \quad – \quad 4.553 \qquad (12)$$

Where Vs is the shear-wave velocity, Qa is the allowable bearing capacity.

Vs30 and site classification

Shear-wave velocity has been utilized as an essential parameter for estimating the dynamic properties of soils since long time. VS30 is known as the average of shear-wave velocity in the top 30 meters, based on travel time from the surface to a depth of 30 m. It is used to classify the soil into six classes (A–F) according to the National Earthquake Hazards Reduction Program [34]. Vs30 can be calculated from Eq. (13).

$$V_s{}^{30} = \frac{30}{\sum_{i=1}^{N}(h_i/v_i)}, \quad (13)$$

where *VI* is shear-wave velocity in m/s, and *hi* is the thickness of any layer (between 0 and 30 m).

Results and Discussion

The integration between electrical, shear wave, and borehole data were used to estimate the dynamic characteristics of the subsurface soil, which could have direct effects on the constructions in the City of Tenth Ramadan. The geoelectrical data included 2-D resistivity data, where Wenner array indicated the vertical variation, while the dipole array reflected the horizontal and vertical variations. The results of inversion show that the dipole sections indicate horizontal variation, as shown in (Figure 4). The subsurface succession consists of two geologic units. The first layer consists of sand, silt, and gravel with low resistivity ranging from 25 to 65.5 ohm m. The thickness of this layer increases toward the south, reaching about 12m at nearest borehole 1. The second layer has moderate resistivity, corresponding to dry sand with gravels and calcareous materials. The thickness of this layer is observed to increase in the center of the section and decreases toward the north nearest borehole 2. It can be distinguished at the depth range from 9m at the north to 12m toward the south.

The data of primary and shear waves obtained from boreholes were used to calculate the different elastic moduli, as listed in (Table 4). The values of Young's modulus (E) ranged

between 0.029 and 0.537 GPa, Bulk modulus (K) range between 0.030 and 0.991 GPa., and shear modulus (μ) or rigidity range between 0.011 and 2.00 Gpa. Poisson's ratio (σ) was
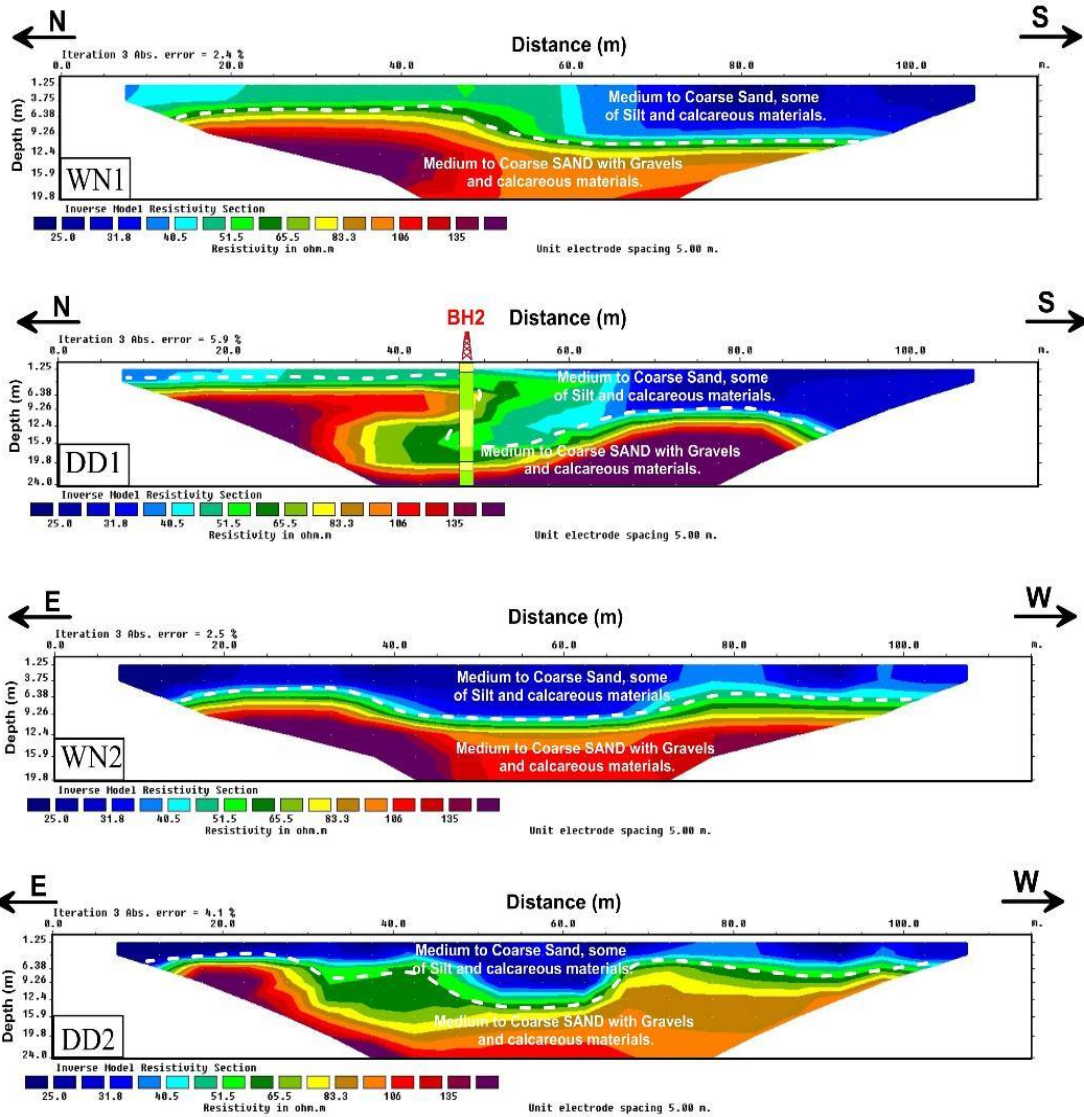
characterized by relative low ratio, ranging between 0.328 and 0.415, revealing that the soils belong to dense granular soil, according to Table 2. SPT value is one of the most important parameters used to determine the mechanical properties of subsurface soil. The N-values ranged from 15.30 to 31.29, which reflects medium to dense cohesionless soil, according to (Table 1).

Figure 4- The 2-D electrical resistivity inverted sections along the profiles of P1, represented by DD1 dipole–dipole
array and WN1 Wenner array and P2, represent by DD2 and WN2.

Table 4- The elastic moduli values based on shear waves measured in boreholes 1 and 2.

Borehole 1										Borehole 2				
Dep.	Vp	Vs	δ	ρ	μ	E	K	E	K	Vp	Vs	δ	ρ	μ
1	195	97	0.336	1.16	11	29	30	56.6	58.9	264	130	0.340	1.25	21.1
2	352	173	0.341	1.34	40	108	113	111.8	116.1	357	176	0.339	1.35	41.7
3	438	208	0.354	1.42	61	166	190	133.7	143.2	390	190	0.344	1.38	49.7
4	495	245	0.338	1.46	88	235	241	195.9	201.7	457	226	0.338	1.43	73.2
5	559	283	0.328	1.51	121	321	310	204.5	223.8	474	229	0.348	1.45	75.9
6	583	287	0.340	1.52	125	336	351	272.1	286.1	532	261	0.342	1.49	101.4
7	614	303	0.339	1.54	142	379	393	292	311.1	551	269	0.344	1.50	108.7
8	642	314	0.343	1.56	154	413	438	319.4	327.1	567	281	0.337	1.51	119.4
9	856	326	0.415	1.68	178	504	991	310.6	324.2	563	277	0.340	1.51	115.9
10	851	324	0.415	1.67	176	498	978	318.4	346.2	576	279	0.347	1.52	118.2
11	647	316	0.343	1.56	157	420	446	346.5	372.3	596	290	0.345	1.53	128.8
12	638	302	0.356	1.56	142	385	445	332.5	367.5	590	284	0.349	1.53	123.2
13	655	311	0.354	1.57	152	411	471	341.2	366.8	592	288	0.345	1.53	126.8
14	658	320	0.345	1.57	161	433	465	341.9	357.8	588	289	0.341	1.53	127.5
15	667	329	0.339	1.58	171	457	474	373.8	400.7	616	300	0.345	1.54	139.0
16	686	337	0.341	1.59	180	483	506	386.1	366.3	604	308	0.324	1.54	145.8
17	682	333	0.343	1.58	176	472	503	430.6	425.3	641	322	0.331	1.56	161.7
18	688	340	0.338	1.59	184	491	507	430.2	423.1	640	322	0.331	1.56	161.7
19	689	340	0.339	1.59	184	492	509	405.9	423.4	634	312	0.340	1.56	151.4
20	695	335	0.349	1.59	179	482	531	416.5	428.9	639	316	0.338	1.56	155.6
21	696	339	0.344	1.60	183	492	527	389.9	386.6	614	308	0.332	1.54	146.4
22	701	343	0.343	1.60	188	504	534	430.7	454.3	653	320	0.342	1.57	160.5
23	701	343	0.343	1.60	188	504	534	430.7	439.7	647	321	0.337	1.56	161.1

24	718	350	0.344	1.60		197	528	565	633	314	0.337	1.55
	153.3	409.9	418.6									
25	718	347	0.348	1.60		193	521	570	646	318	0.340	1.56
	158.0	423.6	441.5									
26	713	351	0.340	1.60		197	529	551	653	324	0.337	1.57
	164.5	439.8	448.9									
27	713	353	0.338	1.60		200	534	548	644	318	0.339	1.56
	157.9	422.8	437.1									
28	717	349	0.345	1.60		195	525	564	664	321	0.348	1.57
	162.1	437.0	477.6									
29	720	353	0.342	1.61		200	537	566	675	327	0.347	1.58
	169.0	455.1	494.7									
30	720	349	0.346	1.61		196	527	572	698	333	0.353	1.59
	176.7	478.0	540.7									

Dep. = depth (m), Vp = P-wave velocity (m/sec), Vs = S-wave velocity (m/sec), σ = Poisson's ratio, ρ = density gm/cm3, m = shear modulus (GPa), E = Young's modulus (GPa), K = bulk modulus (GPa).

The engineering parameters were calculated and the results are summarized in table 5, whereas the complete results are plotted in Figures 5 and 6. Interestingly, when these results were extrapolated, several noteworthy results were found.

The Concentration Index (Ci) value of the soil ranged between 3.41 at the depth of 9m , 4.08 in BH1, and 3.86 to 4.08 in BH2 (Figure 5).
Stress Ratio (Si) values ranged between 0. 505 and 0.710 in BH1and 0.480 to 0.545 in BH2.
The Material Index (Mi) values ranged from -0.41 to -0.31 in BH1and BH2.
Ultimate Bearing Capacity (Qult) values ranged between 459 and 939 in BH1and 568 to 917 in BH2, while the uppermost layers, within 6m, had the lowest values of allowable Bearing Capacity (Qa) and the rest of the layers had the highest values (Figure 6).
N values ranged from 15 to 31.2 in BH1 and 19 to 30.5 in BH2. Most of the upper layers, above 6 m, were characterized by the lowest N values, while these values increased with increasing depth in boreholes (Figures 5 and 6).

Table 5-The calculated geotechnical engineering parameters from two boreholes data.

No. value	Ci		Si		Mi		Qut		Qa		N- Vs30 class
Borehole	Min.	Max.	Min.	Max.	Min.	Max.	Min.	Max.	Min.	Max.	Min. Max.
1	3.82	4.05	0.505	0.71	- 0.41	-0.31	459	939	153	313	15 31.2 320 D
2	3.86	4.o8	0.480	0.545	-o.41	-0.32	568	917	189	306	19 30.5 292 D

Ci = Concentration index, Si = Stress ratio, Mi = Material index, Qult = ultimate bearing capacity (Kg/Cm2), and Qa = allowable bearing capacity (Kg/Cm2).
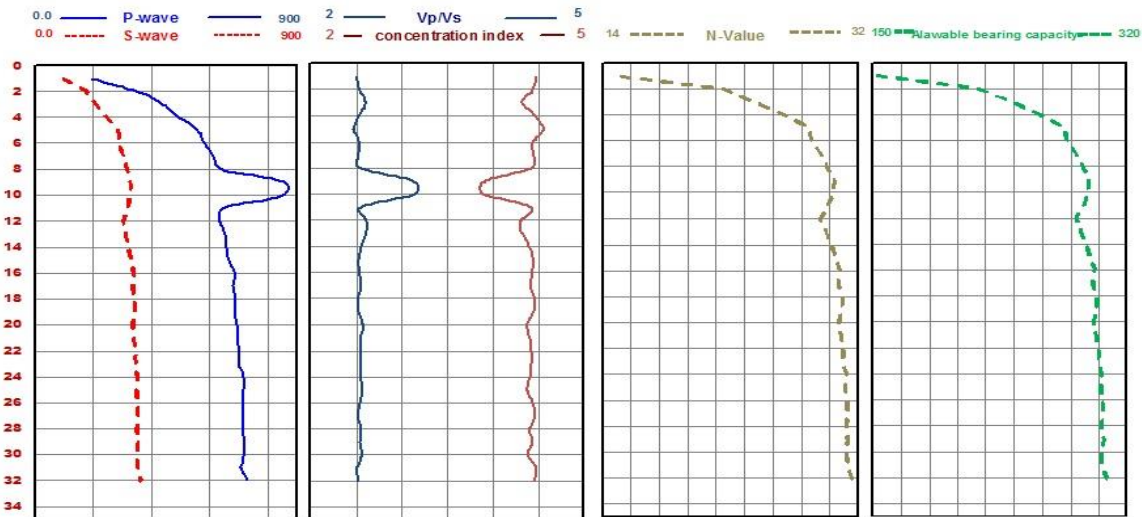
Figure 5- A graph of P and S waves, Vp/Vs, concentration index, N value, and allowable bearing capacity in borehole 1.
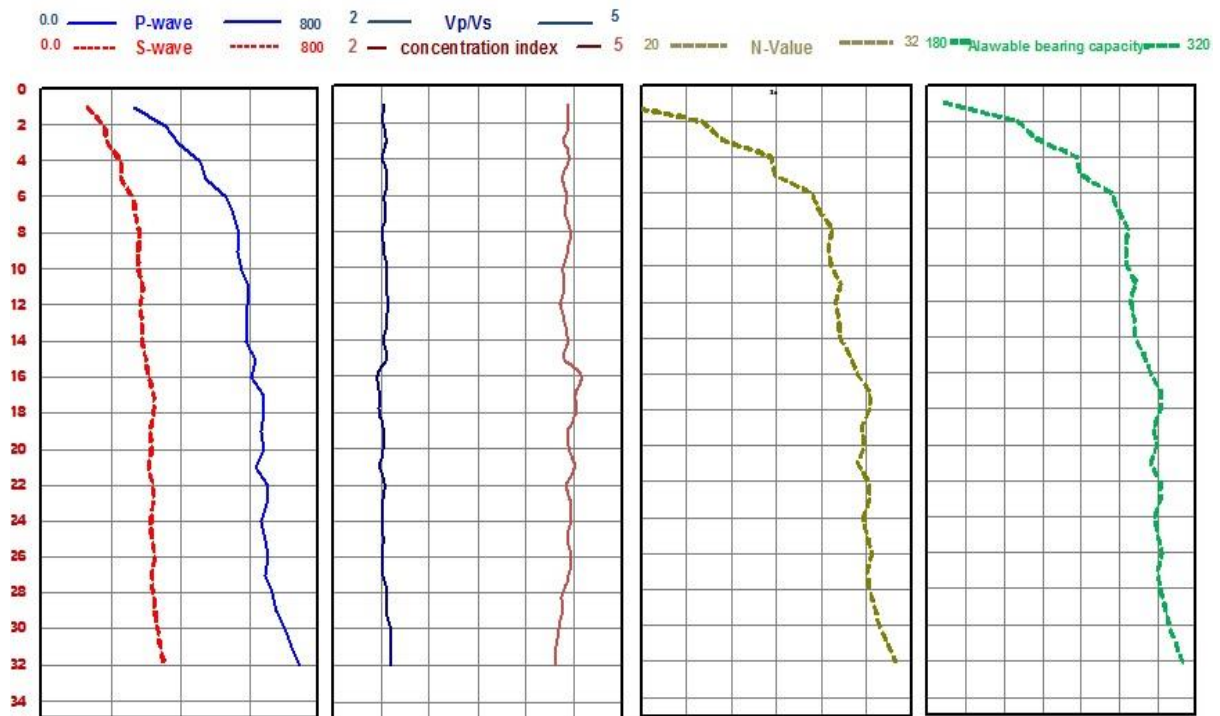

Figure 6 - Shows the graph between P and S waves, Vp/Vs and conc. Index, N value and allowable bearing capacity in borehole 2.

From the obtained results of the resistivity and seismic refraction surveys, a new empirical equation with a high correlation coefficient, $R^2 = 0.9751$, was derived to predict the S-wave (97.5 %) for the bedrock in the study area (Figure 7), as follows:

$$Vs = 1.0302 \, \rho + 172.74 \qquad (12)$$

where Vs is S-wave velocity and ρ is the true resistivity.

This study aids in the estimation and prediction of the properties of the subsurface material (soils and rocks). It is especially useful in reducing the cost of drilling based on

investigation as well as increasing the understanding of the Earth's subsurface geotechnical parameters.
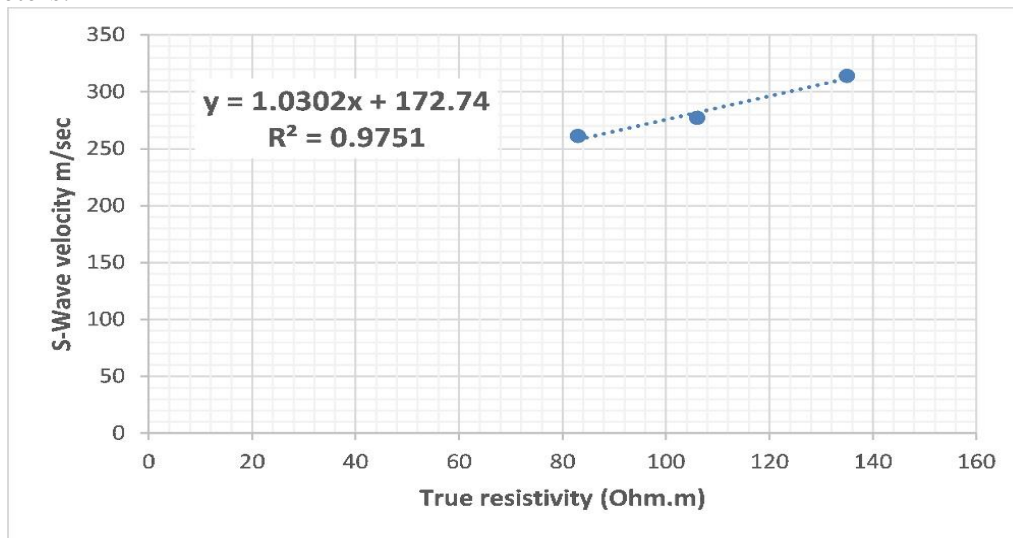

Figure 7- True Resistivity (Ω.m) versus S-wave velocity (m/sec).

The correlation between resistivity, borehole, and down-hole data showed that the subsoil, i.e. less than 8m, has low and variable resistivity and shear wave values. This reflects that the subsurface soil is heterogeneous with low compaction and rigidity. Soil with lower shear wave velocity is lower in bearing capacity [10]. The values of resistivity and shear wave increased from the depth more than 6 m to the end of the borehole. This indicates that the competence and bearing capacity increase, as shown in Figures 5 and 6. In addition, N values increased from top to bottom in the two boreholes. Finally, the NEHRP site classification revealed that soil classes in general reflect sites of class D.

Conclusions

ERT and shear wave data were used to delineate the subsurface soil's structural elements, and calculate the dynamic geotechnical properties of the soil in the Tenth of Ramadan City, which is a suggested site for the construction of factories. The results of the geotechnical properties of the soil and competence scales reveal that the competence of the soil increases with increasing the depth, ranging from fairly to moderately competent material. The integration between the results of ERT, seismic interpretation, and geotechnical properties of soil show that the study site consists of two subsurface layers; the uppermost is weathered soil, with a thickness of 6 m, very low shear wave velocity, lower bearing capacity. The competence of the soil increase at depth more than 6m, characterized by not detectable subsurface structure (fracture or faults). Hence, it is concluded that this site is suitable for constructing factories. The present work can be utilized as a preliminary engineering site investigation technique to mitigate the potential hazards. It was intelligible that the information coming from ERT resistivity inversion and seismic refraction results allow describing the subsurface layers distribution with geoengineering data in a low cost strategy. Finally, the present study aids in the estimation and prediction of geotechnical properties of soils and rocks.

References
[1] Boudreault, J.P.; Dubé J.S.; Chouteau, M.; WiniarskiT. Hardy, É. "Geophysical characterization of contaminated urban fills". *Engineering Geology*, vol. 116, pp. 196–206, 2010.

[2] Araffa, S.A.S., Atya, M., Adel M.E. Mohamed, Mahmoud Gabala, Mohamed Abdel Zaher, Mamdouh, M. Soliman, Hany S. Mesbah, Usama Massoud, Hany M. Shaaban. "Subsurface investigation on Quarter 27 of May15th city, Cairo, Egypt using electrical resistivity tomography and shallow seismic Refraction Techniques". *NRIAG Journal of Astronomy and Geophysics*, 2014.

[3] Othman, A.A.A., "Construed geotechnical characteristics of foundation beds by seismic measurements". *J. Geophys. Eng*. Vol. 2, pp. 126–138, 2005.

[4] Khalil, M.H., Hanafy, S.M. **2008.** "Engineering applications of seismic refraction method: A field example at Wadi Wardan, Northeast Gulf of Suez, Sinai, Egypt". *Journal of Applied Geophysics*, vol. 65, pp. 132- 141, 2008.

[5] Silva, C.P.L. Cartografia Geotécnica Tridimencional do Setor Noroeste de Brasília. Publicação G.TD 072/2011. Universidade de Brasília – UnB, Brasília, 299p. Tese (Doutorado), Departamento de Engenharia Civil Ambiental, 2011.

[6] Attwa M, El Shinawi A. Geoelectrical and geotechnical investigations at tenth of Ramadan City, Egypt—a structure based (SB) model application. Near surface geoscience 2014-20th European meeting of environmental and engineering geophysics, 2014.

[7] Eleraki, M., M. Gadallah, K. Gemail and M. Attwa, "Application of resistivity method in environmental study of the appearance of soil water in the central part of Tenth of Ramadan City, Egypt". Quarterly. *Journal of Engineering Geology and Hydrology*, vol. 43, pp. 171–184, 2010.

[8] Shebl S, Gemail KS, Attwa M, Soliman SA, Azab AA, Farag MH, "Utilizing shallow seismic refraction indefining the geotechnical properties of the foundation materials: a case study at New Minia City, Nile Valley", *Egypt. J Pet*. vol. 28, pp. 145–154, 2019.

[9] Gemail K.S., Shebl Salah, Attwa M., Soliman Shokry A., Azab Ahmed, Farag M.H. " Geotechnical assessment of fractured limestone bedrock using DC resistivity method: a case study at New Minia City, Egypt", *NRIAG Journal of Astronomy and Geophysics*, vol. 9, no. 1, pp. 272- 279, 2020.

[10] Kramer, Steven L. *Geotechnical Earthquake Engineering, Prentice Hall*, 1996, p. 653.

[11] Said, R. *The Geology of Egypt. Elsevier, Amsterdam*, 1990.

[12] CONCO, Geological map of Egypt. Scale 1:500 000; Sheet Cairo. CONCO and the Egyptian General Petroleum Corporation, Cairo, 1987.

[13] El-Kadi, F. A, Drilling and Geotechnical investigation at the Tenth of Ramadan City, Cairo, Egypt. El Nile Engineering Consulting Office, Internal Report, 2019.

[14] Perrone A., Iannuzzi A. et al., "High-resolution electrical imaging of the Varco d'Izzo earthflow (southern Italy)". *J Appl Geophys*, vol. 56, no. 1, pp. 17–29, 2004.

[15] Loke, M.H, Tutorial: 2-D and 3-D electrical imaging surveys. Penang, Universiti Sains Malaysia, unpublished course notes. World Wide Web Address: www. Geoelectrical com., 2020.

[16] Geotomo . Manual RES2DINV Ver. 3.4. **2006**. Penang, Malaysia, Geotomo Software, 132 p.

[17] Loke, M. H., and Barker, R. D., "Rapid least-squares inversion of apparent resistivity pseudosection by a quasi-Newton method". *Geophys. Prospect.*, vol. 44, pp. 131-152, 1996.Sasaki, Y. "Resolution of resistivity tomography inferred from numerical simulation", *Geophysical Prospecting*, vol. 40, pp. 453-464, 1992.

[18] Gretener, P. **2003**. Summary of the Poisson's Ratio debate 1990–2003. Feature Article, CSEG Recorder.28, 44-45.

[19] Salem, H. The theoretical and Practical Study of Petrophysical, Electric and Elastic Parameters of Sediments, Germany, Kiel Insitut for Geophysik. Ph.D.thesis, 1990.

[20] Telford, W.M., Sheriff, R.E., *Applied geophysics, Cambridge university press*, 1990.

[21] Toksöz, M.N., Cheng, C.H., Timur, A. "Velocities of seismic waves in porous rocks", *Geophysics*, vol. 41, pp. 621-645, 1976.

[22] Keceli, A. "Soil parameters which can be determined with seismic velocities", *TMMOB Jeofizik Mühendisleri Odası, Jeofizik*, vol. 16, pp. 17-29, 2012.

[23] Lowrie, W**.,** *Fundamentals of geophysics. Cambridge University Press*, 2007.

[24] Mott, P., Dorgan, J., Roland, C.**,** "The bulk modulus and Poisson's ratio of "incompressible" materials". *Journal of Sound and Vibration,* vol. 312, pp. 572-575, 2008.

[25] Sivrikaya O and Toğrol E., "Determination of undrained strength of fine-grained soils by means of SPT and its application in Turkey". *Eng Geol*. vol. 86, pp. 52–69, 2006.

[26] Anbazhagan P, Parihar A and Rashmi H N., "Review of correlations between SPT N and shear modulus: a new correlation applicable to any region Soil Dyn". *Earthq. Eng*., vol. 36, pp. 52–69, 2012.

[27] Stuempel H, Kahler S, Meissner R and Milkereit B., "The use of seismic shear waves and compressional waves for lithological problems of shallow sediments Geophys". *Prospect*., vol. 32, pp. 662–75, 1984.

[28] Bowles, J. E. *Physical and Geotechnical Properties of Soils*, *London: McGraw-Hill*, 1984.

[29] Das, B. M. *Principles of Geotechnical Engineering. PWS Publishing Company*, 1994.

[30] Matasovic N, Kavazanjian E Jr., "Cyclic characterization of oil landfill solid waste". *J Geotech Geoenviron Eng ASCE.*, vol. 124, no. 3, pp. 197–210, 1998.

[31] Sheriff, R.E. and Geldart, L.P., *Exploration Seismology, Cambridge Univ. Press, Cambridge*, 1986, p. 316.

[32] Parry, R.H.G. Estimating bearing capacity of sand from SPT values JGED ASCE 103: Gt.9, pp. 1014–1043, 1977.

[33] BSSC NEHRP, Recommended Provisions for seismic Regulations for New buildings and Other Structures, Part1: Provisions, FEMA 368, Federal Emergency Management Agency, Washington, D.C., 2003.